Theranostic Nanoparticles

Deutsche Ausgabe: DOI: 10.1002/ange.201602188
Internationale Ausgabe: DOI: 10.1002/anie.201602188

Cell-Penetrating Poly(disulfide) Assisted Intracellular Delivery of Mesoporous Silica Nanoparticles for Inhibition of miR-21 Function and Detection of Subsequent Therapeutic Effects

*Changmin Yu, Linghui Qian, Jingyan Ge, Jiaqi Fu, Peiyan Yuan, Samantha C. L. Yao, and Shao Q. Yao**

Abstract: *The design of drug delivery systems capable of minimal endolysosomal trapping, controlled drug release, and real-time monitoring of drug effect is highly desirable for personalized medicine. Herein, by using mesoporous silica nanoparticles (MSNs) coated with cell-penetrating poly(disulfide)s and a fluorogenic apoptosis-detecting peptide (DEVD-AAN), we have developed a platform that could be uptaken rapidly by mammalian cells via endocytosis-independent pathways. Subsequent loading of these MSNs with small molecule inhibitors and antisense oligonucleotides resulted in intracellular release of these drugs, leading to combination inhibition of endogenous miR-21 activities which was immediately detectable by the MSN surface-coated peptide using two-photon fluorescence microscopy.*

In recent years, mesoporous silica nanoparticles (MSNs) have found promising applications in biomedicine as a multifunctional drug-delivery platform owing to their desirable properties, including high surface areas, uniform pore sizes, high loading capacity, easy functionalization, and nontoxicity.[1] An ideal "magic bullet" based on MSNs would require such a system to be capable of specific targeting of diseased cells/tissues, efficient transfer of payloads across the cell membrane, minimal endolysosomal trapping, controlled release of drugs in response to intracellular stimuli, and spontaneous detection of drug effects. These criteria are necessary to develop theranostic nanomedicines for personalized treatment.[2] To date, numerous MSN-based delivery systems making use of different capping strategies to achieve intracellular controlled release of drugs have been reported.[3] Among them, nucleic acid-capped MSNs stand out as they offer a sequence-dependent universal strategy for drug release.[4] By using antisense oligonucleotide (ASO)-capped MSNs, we recently reported a system capable of intracellular controlled release of small-molecule drugs in a manner dependent upon the endogenous expression of microRNAs (i.e. miR-122).[5] MicroRNAs are small regulatory noncoding RNAs that control about 30% of human genes as well as many biological processes associated with cancer, cardiovascular diseases, neurological disorders, and viral infection.[6]

Significant obstacles remain for current MSNs to be used as an ideal drug-delivery system. First, in order to enter mammalian cells, MSNs are normally surface-modified with cell-penetrating peptides (CPPs) or cationic polymers, and subsequently uptaken by cells by endocytosis.[1,3,4,7] Once inside cells, endolysosomal escape may occur but does so poorly, resulting in slow and highly variable cargo release.[7] Furthermore, positive surface charges on such MSNs often cause unwanted cytotoxicity, poor serum stability, and rapid uptake by the reticuloendothelial system, thus limiting their in vivo therapeutic efficacy. The development of novel endocytosis-independent MSN delivery systems is therefore needed. On the other hand, to evaluate the therapeutic effect of an intracellularly released drug from the nanoparticles, theranostic MSNs often use intrinsic fluorescence of the drug (i.e. Doxorubicin, or Dox) to track its subcellular localization, but such approaches are highly limited as most drugs do not have any traceable fluorescence.[8,9] An ideal theranostic system should monitor the drug's biological effects instead of its release. Herein, we report a new MSN-based drug delivery system that has effectively solved both challenges; by capping nanoparticles with cell-penetrating poly(disulfide)s,[10] and a fluorogenic apoptosis-detecting peptide (DEVD-AAN), we have successfully created theranostic MSNs that were uptaken rapidly by mammalian cells via endocytosis-independent pathways. Subsequent intracellular release of loaded drugs that target endogenous miR-21 (a microRNA highly expressed in a variety of cancers),[11] and more importantly their theranostic effects, were successfully detected by monitoring the ensuing drug-induced apoptosis. This was achieved in real time by two-photon fluorescence microscopy. Since many anticancer drugs cause tumors to undergo apoptosis,[12] our strategy is therefore well-suited for a variety of biomedical applications.

Cell-penetrating poly(disulfide)s (CPDs) are synthetic mimics of poly-arginine CPPs in which the polypeptide backbone was replaced with poly(disulfide)s.[10,13] They are characterized by rapid cellular uptake, minimal cytotoxicity, and efficient cytosolic degradation/cargo release triggered by

[*] Dr. C. Yu, L. Qian, Dr. J. Ge, J. Fu, Dr. P. Yuan, S. C. L. Yao, Prof. Dr. S. Q. Yao
Department of Chemistry
National University of Singapore
3 Science Drive 3, Singapore 117543 (Singapore)
E-mail: chmyaosq@nus.edu.sg
Dr. C. Yu
College of Materials Science & Engineering
South China University of Technology
Guangzhou (China)
Dr. J. Ge
Institute of Bioengineering, Zhejiang University of Technology
Hangzhou (China)

Supporting information for this article can be found under: http://dx.doi.org/10.1002/anie.201602188.

endogenous glutathione (GSH, known to be highly expressed in tumor cells).[14] Recent studies showed that large CPD-conjugated cargos, such as proteins, could be rapidly delivered to mammalian cells with no apparent endolysosomal trapping.[10,13b] Whether or not the same holds true for CPD-coated nanomaterials (i.e. MSNs) is, however, not known. In our drug delivery system, phosphonate-modified nanoparticles were first loaded with a small-molecule drug (Scheme 1).

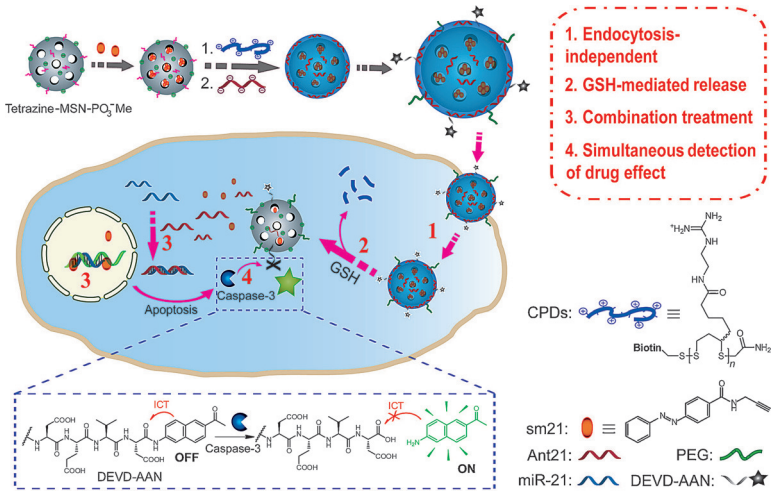

Scheme 1. Schematic representation of the CPD-capped MSNs with self-reporting DEVD-AAN to detect caspase-3/-7-induced apoptosis in cancer cells upon GSH-triggered release and combination treatment of cargos (small molecule + Ant21). The fluorescence Turn-ON property of DEVED-AAN is controlled by intramolecular charge transfer (ICT).[16] See Supporting Information for other chemical structures.

Subsequent capping with positively charged CPDs via charge–charge interaction, followed by loading of a second ASO-based, negatively charged Ant21 (antagomir of miR-21 or *anti*-miR-21), provided the corresponding drug-loaded MSNs named CPD-MSN-Ant21. Finally, the surface of MSNs was modified with a polyethylene glycol (PEG)-linked fluorogenic peptide DEVD-AAN via the tandem bioorthogonal tetrazine-TCO ligation and copper-free DBCO-azide click chemistry.[15] DEVD-AAN is a caspase-responsive probe capable of two-photon Turn-ON fluorescence imaging of cell apoptosis induced by caspase-3/-7 activation (an event caused by many anticancer drugs).[16] As shown in Scheme 1, key steps in this novel theranostic delivery system involve: 1) CPD-assisted intracellular delivery of MSNs; 2) CPD depolymerization triggered by endogenous GSH; 3) cytosolic release of both Ant21 and the small-molecule drug leading to combination inhibition of miR-21 function; and 4) real-time in situ imaging of cell apoptosis from the MSN-bound self-reporting DEVD-AAN.

To prepare our delivery system, phosphonate-modified nanoparticles were first synthesized.[17] The resulting MSNs were highly monodisperse (mean diameter: ca. 105 nm) and possessed well-defined pore sizes (ca. 3.2 nm) with high specific areas (Figures S3,S4). Next, the intrinsically fluorescent Dox was loaded as a model cargo to directly measure drug loading/controlled release processes in vitro. The loading capacity of Dox was determined to be 131.1 $\mu mol\,g^{-1}$ (Figure S5). Upon CPD capping and Ant21 loading, followed by PEG modification, the resulting CPD-MSN-Dox-Ant21 showed minimal aggregation in cell culture containing 10% fetal bovine serum (FBS; 24 h) and negligible cargo leakage under physiological conditions. Next, in a DNA gel retardation assay, GSH-dependent controlled release of Dox/Ant21 was successfully demonstrated (Figure S6,S7); the in vitro release of both drugs increased in a time-dependent manner with increasing concentrations of either GSH or HeLa cell lysates. Pretreatment of the MSNs with *N*-ethylmaleimide (NEM, a GSH blocker) led to significant reduction in drug release. Therefore, in most cancer cells where elevated levels of endogenous GSH are known,[14] our MSNs were expected to release the payloads efficiently. This is different from our previously developed MSNs in which controlled release of payloads occurred only in cells (e.g. hepatocellular carcinoma) that have high expression levels of miR-122.[5]

Next, confocal laser scanning microscopy (CLSM) was performed on FITC-doped MSNs for convenient assessment of cellular uptake and subcellular distribution of these CPD-capped MSNs in live HeLa cells (CPD-MSN-Ant21 & CPD-MSN; Figure 1 and Figures S8–S10). Negative control MSNs (i.e. MSN-PO_3^-Me without CPD capping), as well as amine-modified positively charged MSNs (MSN-RGD and MSN-NH_2) which were previously shown to be uptaken by cells via endocytosis-dependent pathways,[5,7] were simultaneously investigated by real-time imaging experiments (see Supporting Videos). As shown in Figure 1 a, in as short as 30 min, most CPD-MSN-Ant21 had accumulated around the cell membrane, and in the following 60 min, the nanoparticles continuously crossed the cell membrane and were distributed evenly throughout the cytosol, with no evidence of being trapped inside endolysosomal vesicles (colored in red). When compared to CPD-conjugated proteins which took <30 min for complete cell uptake,[10] we noted these CPD-capped MSNs needed a longer time to enter cells, presumably due to their significantly larger sizes. For the same reason, none of the internalized MSNs entered cell nucleus (colored in blue), which has its own membrane and limited pore size.[18] On the contrary, negatively charged, uncapped MSNs (MSN-PO_3^-Me) did not enter cells even after prolonged incubation (12 h, Figure S8). Both CPD-MSN-Ant21 and CPD-MSN (not capped with Ant21) displayed similar cell uptake kinetics and subsequent cellular distributions (Figure S9). The amine-modified MSNs (MSN-RGD and MSN-NH_2) showed much slower cell uptake with most of them ending up inside endolysosomal vesicles after 6 h incubation (Figures 1 b–d, Figure S10); quantitative co-localization analysis of the successfully internalized MSNs with both LysoTracker (a lysosome stain) and Dextran Red (an endosome stain) clearly showed the superiority of our CPD-capped MSNs as novel systems over existing nanoparticles for intracellular drug delivery with minimal endolysosomal trapping. To unequivocally establish the endocytosis-independent cell uptake of

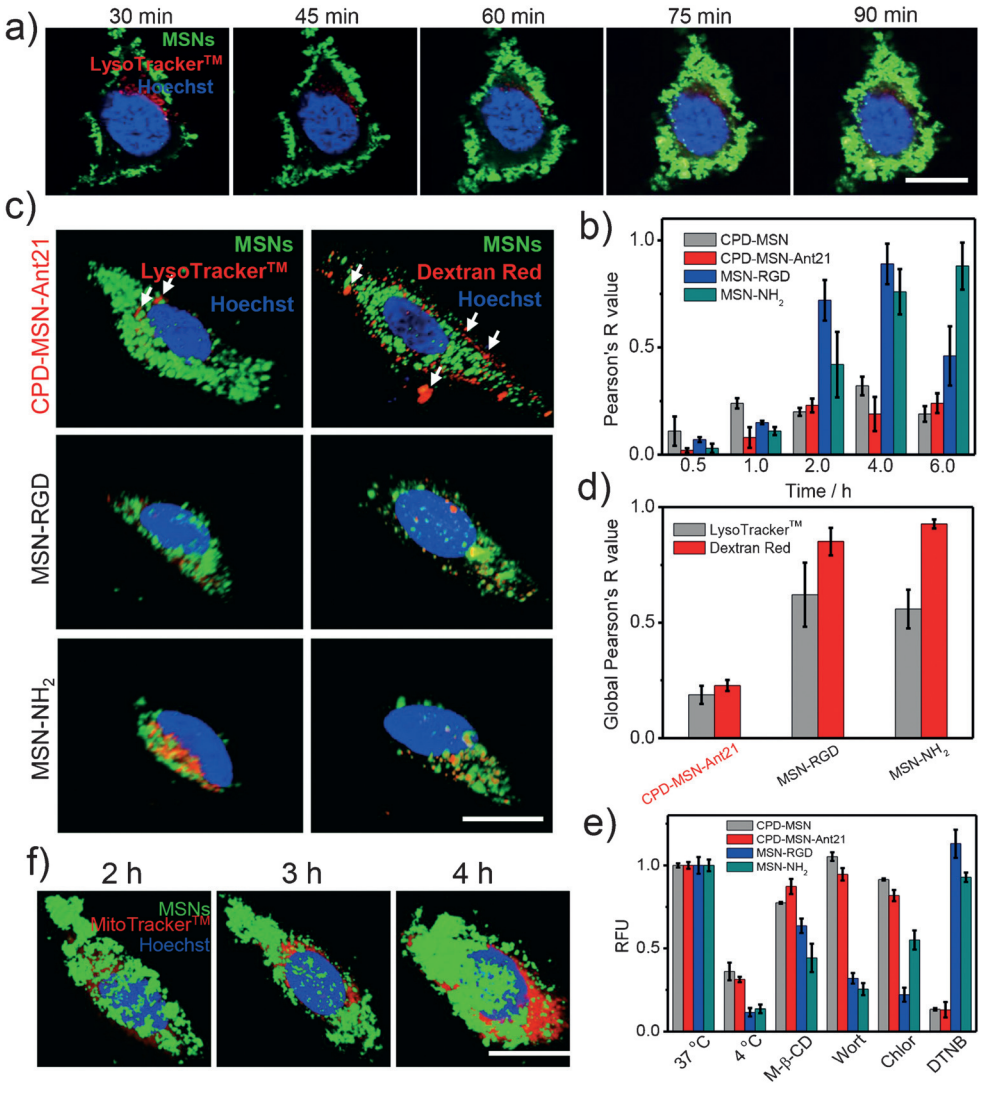

Figure 1. a) CLSM of live HeLa cells treated with FITC-doped CPD-MSN-Ant21 (10 μg mL^{-1}; in green). Cells were stained with LysoTracker (red) and Hoechst (blue). b) Pearson co-localization analysis of different MSNs with LysoTracker at different incubation times. Data obtained from Figure S9 by using image J software. Error bars were obtained by analysis of two different cells. Global Pearson's *R* values were calculated with VOLOCITY software. c) 3D projections showing *Z*-stack images at 45° view (step size, 0.163 μm) of HeLa cells incubated with different MSNs (2 h for CPD-MSN-Ant21 and 4 h for MSN-RGD and MSN-NH_2), followed by staining with either LysoTracker (left) or Dextran Red (right). d) Co-localization analysis of the different channels in (c). e) Fluorescence quantification of cell uptake by different MSNs (10 μg mL^{-1}; 2 h incubation at 37 °C) in HeLa cells treated with endocytosis inhibitors, including methyl-β-cyclodextrin (M-β-CD), wortmannin (Wort), chlorpromazine (Chlor). Similar experiments were performed at 4 °C (no inhibitor) or in the presence of DTNB. Data were normalized to cells treated only with each type of MSNs at 37 °C. f) 3D projections showing *Z*-stack images (step size, 0.163 μm) of HeLa cells treated with CPD-MSN-Mito-Ant21 (10 μg mL^{-1}) at different time points. MitoTracker (Red). Scale bar = 20 μm.

CPD-capped MSNs, we carried out detailed uptake studies in HeLa cells at different temperatures and in the presence of endocytosis inhibitors including chlorpromazine, wortmannin and methyl-β-cyclodextrin (Figures 1 e and Figure S11); unlike MSN-RGD and MSN-NH_2, uptake of both CPD-MSN and CPD-MSN-Ant21 were insensitive to endocytosis inhibitors. Reduced temperature decreased the cell uptake efficiency on all tested MSNs but did not block the process completely. Interestingly, blocking exofacial thiols on the cell surface with 5,5′-dithiobis-2-nitrobenzoic acid (DTNB) significantly suppressed the cell uptake efficiency of CPD-capped MSNs but not other MSNs (i.e. MSN-RGD and MSN-NH_2), clearly supporting a thiol-mediated cargo delivery mechanism as previously reported.[10,13] We further confirmed the endocytosis-independent delivery of these CPD-capped MSNs did not cause nonspecific membrane disruption (Figure S12; done with CPD-MSN-21C—control nanoparticles coated with 21C oligo), and occurred in a variety of other mammalian cell lines (Figure S13). Finally, to monitor the intracellular release of payloads from these CPD-capped MSNs, we carried out imaging experiments with live HeLa cells treated with FITC-doped CPD-MSN-Mito-Ant21 (loaded with MitoTracker as a model drug; Figure 1 f); the 3D projections of *Z*-stack images after different incubation time points (2–4 h) clearly indicated the successful cytosolic release of free MitoTracker (colored in red) and its subsequent localization inside mitochondria. The FITC-doped MSNs (colored in green, Figure 1 f), on the other hand, remained in the cytosol because of their large sizes.[5]

Having successfully demonstrated the excellent cell uptake efficiency and GSH-responsive drug release of our newly developed CPD-capped MSNs, we prepared CPD-MSN-sm21-Ant21 and used them for simultaneous co-delivery of two mechanistically distinct inhibitors to achieve combination inhibition of endogenous miR-21 function. As a key oncogenic miRNAs, miR-21 is overexpressed in many types of cancers, and being investigated as a potential therapeutic target for cancer.[11,19] Direct links between its expression and cancer-related processes such as proliferation, migration and tumor growth indicate that miR-21 inhibition activates cell apoptosis which may lead to eventual eradication of tumor cells.[11,20] In our strategy, Ant21, a chemically modified ASO which contains phosphorothioates in place of

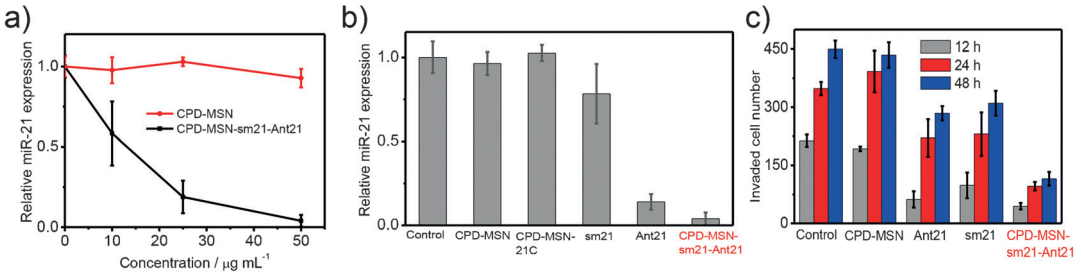

Figure 2. a) *q*PCR determination of endogenous miR-21 expression levels from HeLa cells treated with different concentrations of CPD-MSN-sm21-Ant21 and CPD-MSN for 24 h. b) Graphical summary of (a) with other control MSNs (all at 50 μg mL^{-1}), or Ant21 or sm21 only (150 nM and 4.5 μM, respectively). RLU was normalized to the control (cells treated with DMSO). c) Analysis of migration of HeLa cells after treatment with MSNs (50 μg mL^{-1}) or an inhibitor (150 nM Ant21 or 4.5 μM sm21, respectively) for different time (12–48 h); see Figure S14 for details.

the normal phosphodiester linkage in the oligonucleotide backbone with periodic insertion of 2′-methoxy nucleotides, was chosen, because of its excellent intracellular stability and improved binding affinity toward miR-21.[21] A novel compound, sm21, which was shown to inhibit endogenous miR-21 activity by blocking the synthesis of pri-miRNA-21,[22] was used as the small-molecule inhibitor (Scheme 1). We previously showed combination inhibition of miR-122 (a microRNA involved in *Hepatitis C* virus infection and liver cancer) with MSNs loaded with small molecules and ASOs could effectively inhibit cellular miRNA activities.[5] In CPD-MSN-sm21-Ant21, the capping CPD not only served as a carrier capable of endocytosis-independent MSN delivery as earlier demonstrated, it was also used as gatekeeper to control the intracellular release of both the encapsulated sm21 and the surface-bound Ant21. Upon MSN cell uptake, millimolar concentrations of endogenous GSH inside most cancer cells would ensure rapid and efficient release of both drugs.

In real-time quantitative PCR (*q*PCR) experiments of HeLa cells treated with CPD-MSN-sm21-Ant21, we observed effective combination inhibition of endogenous miR-21 function in dose-dependent manner (Figure 2a,b); no inhibition was observed with control MSNs (e.g. CPD-MSN and CPD-MSN-21C). Inhibition of endogenous miR-21 was previously shown to suppress cancer cell migration and invasion.[11] In a wound-healing and matrigel invasion assay with HeLa cells treated with our drug-loaded MSNs, down-regulation of endogenous miR-21 followed by concurrent inhibition of cell migration/invasion was observed (Figures 2c, S14). These results thus clearly indicate that our single-vehicle system could serve as a robust platform for effective intracellular drug delivery/release and combination inhibition of endogenous miR-21 with two mechanistically distinct inhibitors. The generality of our MSNs for delivery of other drugs with Ant21 was further confirmed from HeLa cells treated with the earlier prepared CPD-MSN-Dox-Ant21 (payloads: Dox + Ant21; Figure S15); these nanoparticles also showed potent inhibitory activities against endogenous miR-21, presumably caused by the general cell-killing effect of Dox (a DNA alkylating agent) and Ant21 inhibition of miR-21. With the intrinsic fluorescence of Dox, we were able to track the intracellular release of Dox and its subsequent localization to the nucleus.

Novel strategies capable of real-time monitoring of delivered drugs' therapeutic effects offer significant advantages over most existing theranostic methods in which release of the drug, rather than its ensuing biological effects in host cells, is evaluated.[24] Inhibition of endogenous miR-21 improves the therapeutic effects of anticancer drugs through induction of apoptosis in solid tumors and hematological malignancies.[11] In addition, many anticancer drugs on the market kill tumors by directly causing cancer cell apoptosis.[12] We therefore envisaged a novel theranostic platform could be developed by directly coupling the surface of CPD-capped MSNs with DEVD-AAN (to detect caspase-3/-7 activation in apoptotic cells), giving CPD-MSN-sm21-Ant21-AAN. As shown in Figure 3a, in a two-photon fluorescence microscope, HeLa cells treated with these self-reporting MSNs started to develop apparent fluorescence after 6 h incubation (through released AAN[23]), and the fluorescence signals increased over the next 18 h, with apparent rounding in the cell morphology (a sign of apoptosis). In contrast, neither fluorescence nor cell

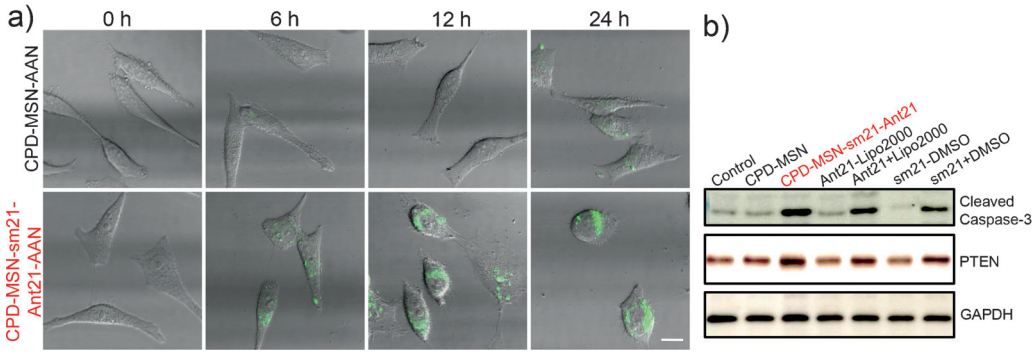

Figure 3. a) Two-photon imaging showing apoptosis of HeLa cells caused by inhibition of miR-21 function with our self-reporting MSNs (50 μg mL^{-1}). Scale bar = 20 μm. b) WB analysis of cleaved caspase-3 and PTEN in HeLa cells treated with different MSNs (50 μg mL^{-1}) or small molecules (150 nM Ant21 or 4.5 μM sm21) for 24 h.

morphological changes was observed in control cells treated with CPD-MSN-AAN (no loaded drugs). Further confirmation of caspase-3/-7 activation was carried out by Western blotting (WB) analysis (Figure 3b); in addition to successful detection of cleaved casapse-3, we also detected a marked increase in the expression of PTEN, a protein previously known to be up-regulated in response to miR-21 inhibition.[25] Interestingly, no miR-21 inhibitory effect was observed in cells treated with either sm21 (no DMSO) or Ant21 (no transfection reagents) alone, clearly indicating the importance of our MSNs as an effective drug delivery platform.

Inhibition of miR-21 by antagomirs was previously found to affect kinase signaling pathways in cardiac fibroblasts, leading to up/down regulation of important enzymes including kinases and poly(ADP-ribose)polymerase-1 (PARP-1).[11] To extend our current system for combination inhibition of miR-21 and its downstream targets, we prepared CPD-MSN-Ant21 encapsulated with different inhibitors of kinases (gefitinib and dasatinib) and PARP-1 (olaparib). The corresponding MSNs were incubated with HeLa cells for 24 h, followed by live-cell imaging, *q*PCR determination of endogenous miR-21 levels, XTT cell viability assays and WB analysis (Figures S16); all results indicate the successful co-delivery of Ant21 and small molecule drugs and subsequent cellular inhibition with our CPD-capped drug delivery system. Caspase-3 activation from the MSN-bound DEVD-AAN was successfully detected as well.

In summary, with cell-penetrating poly(disulfide)s as both a gatekeeper and carrier, a novel MSN-based drug delivery system has been developed, and for the first time, this system showed key advantages of rapid cell uptake with no apparent endolysosomal trapping, intracellular controlled release of payloads triggered by endogenous stimuli, and combination inhibition of endogenous miR-21 with antagomir and different small-molecule inhibitors. Endowed with a self-reporting module capable of sensitive detection of endogenous caspase-3/-7 activation, our theranostic system directly monitored the biological effects of released drugs in real-time. By having successfully solved two critical problems in nanoparticle-based drug delivery systems, this newly developed platform brings us one step closer to the development of personalized medicines for different biomedical applications.

Acknowledgements

Funding was provided by the National Medical Research Council (CBRG/0038/2013) and the Ministry of Education (MOE2012-T2-2-051 and MOE2013-T2-1-048).

Keywords: cell-penetrating poly(disulfide) · drug delivery · endocytosis · nanoparticles · small-molecule inhibitor

How to cite: *Angew. Chem. Int. Ed.* **2016**, *55*, 9272–9276
Angew. Chem. **2016**, *128*, 9418–9422

[1] a) E. Aznar, M. Oroval, L. Pascual, J. R. Murguia, R. Martinez-Manez, F. Sancenon, *Chem. Rev.* **2016**, *116*, 561–718; b) Z. Li, J. C. Barnes, A. Bosoy, J. F. Stoddart, J. I. Zink, *Chem. Soc. Rev.* **2012**, *41*, 2590–2605.
[2] D. Peer, J. M. Karp, S. Hong, O. C. Farokhzad, R. Margalit, R. Langer, *Nat. Nanotechnol.* **2007**, *2*, 751–760.
[3] N. Song, Y.-W. Yang, *Chem. Soc. Rev.* **2015**, *44*, 3474–3504.
[4] C.-H. Lu, I. Willner, *Angew. Chem. Int. Ed.* **2015**, *54*, 12212–12235; *Angew. Chem.* **2015**, *127*, 12380–12405.
[5] C. Yu, L. Qian, M. Uttamchandani, L. Li, S. Q. Yao, *Angew. Chem. Int. Ed.* **2015**, *54*, 10574–10578; *Angew. Chem.* **2015**, *127*, 10720–10724.
[6] a) W. Filipowicz, *Cell* **2005**, *122*, 17–20; b) G. A. Calin, C. M. Croce, *Nat. Rev. Cancer* **2006**, *6*, 857–866.
[7] a) T. Xia, M. Kovochich, M. Liong, H. Meng, S. Kabehie, S. George, J. I. Zink, A. E. Nel, *ACS Nano* **2009**, *3*, 3273–3286; b) S. B. Hartono, W. Gu, F. Kleitz, J. Liu, L. He, A. P. J. Middelberg, C. Yu, G. Q. Lu, S. Z. Qiao, *ACS Nano* **2012**, *6*, 2104–2117; c) J. L. Townson, Y. Lin, J. O. Agola, E. C. Carnes, H. S. Leong, J. D. Lewis, C. L. Haynes, C. J. Brinker, *J. Am. Chem. Soc.* **2013**, *135*, 16030–16033.
[8] K. T. Nguyen, Y. L. Zhao, *Acc. Chem. Res.* **2015**, *48*, 3016–3025.
[9] P. Zhang, F. Cheng, R. Zhou, J. Cao, J. Li, C. Burda, Q. Min, J. Zhu, *Angew. Chem. Int. Ed.* **2014**, *53*, 2371–2375; *Angew. Chem.* **2014**, *126*, 2403–2407.
[10] J. Fu, C. Yu, L. Li, S. Q. Yao, *J. Am. Chem. Soc.* **2015**, *137*, 12153–12160.
[11] V. Jazbutyte, T. Thum, *Curr. Drug Targets* **2010**, *11*, 926–935.
[12] G. Lessene, P. E. Czabotar, P. M. Colman, *Nat. Rev. Drug Discovery* **2008**, *7*, 989–1000.
[13] a) G. Gasparini, E.-K. Bang, J. Montenegro, S. Matile, *Chem. Commun.* **2015**, *51*, 10389–10402; b) G. Gasparini, S. Matile, *Chem. Commun.* **2015**, *51*, 17160–17162.
[14] P. Kuppusamy, H. Li, G. Ilangovan, A. J. Cardounel, J. L. Zweier, K. Yamada, M. C. Krishna, J. B. Mitchell, *Cancer Res.* **2002**, *62*, 307–312.
[15] a) E. M. Sletten, C. R. Bertozzi, *Angew. Chem. Int. Ed.* **2009**, *48*, 6974–6998; *Angew. Chem.* **2009**, *121*, 7108–7133; b) R. Selvaraj, J. M. Fox, *Curr. Opin. Chem. Biol.* **2013**, *17*, 753–760.
[16] M. Hu, L. Li, H. Wu, Y. Su, P.-Y. Yang, M. Uttamchandani, Q.-H. Xu, S. Q. Yao, *J. Am. Chem. Soc.* **2011**, *133*, 12009–12020.
[17] Y.-L. Zhao, Z. Li, S. Kabehie, Y. Y. Botros, J. F. Stoddart, J. I. Zink, *J. Am. Chem. Soc.* **2010**, *132*, 13016–13025.
[18] L. Pan, Q. He, J. Liu, Y. Chen, M. Ma, L. Zhang, J. Shi, *J. Am. Chem. Soc.* **2012**, *134*, 5722–5725.
[19] a) R. Kuner, J. C. Brase, H. Sueltmann, D. Wuttig, *Methods* **2013**, *59*, 132–137; b) L. F. Sempere, et al., *Cancer Res.* **2007**, *67*, 11612–11620.
[20] a) M. D. Jansson, A. H. Lund, *Mol. Oncol.* **2012**, *6*, 590–610; b) Z. X. Wang, B. B. Lu, H. Wang, Z. X. Cheng, Y. M. Yin, *Arch. Med. Res.* **2011**, *42*, 281–290; c) Z. L. Liu, H. Wang, J. Liu, Z. X. Wang, *Mol. Cell. Biochem.* **2013**, *372*, 35–45.
[21] J. Li, S. Tan, R. Kooger, C. Zhang, Y. Zhang, *Chem. Soc. Rev.* **2014**, *43*, 506–517.
[22] K. Gumireddy, D. D. Young, X. Xiong, J. B. Hogenesch, Q. Huang, A. Deiters, *Angew. Chem. Int. Ed.* **2008**, *47*, 7482–7484; *Angew. Chem.* **2008**, *120*, 7592–7594.
[23] L. Li, H. Wijayal, S. Samanta, Y. Lam, S. Q. Yao, *Sci. Rep.* **2015**, *5*, 11522.
[24] H. Mekaru, J. Lu, F. Tamanoi, *Adv. Drug Delivery Rev.* **2015**, *95*, 40–49.
[25] F. Meng, R. Henson, H. Wehbe-Janek, K. Ghoshal, S. T. Jacob, T. Patel, *Gastroenterology* **2007**, *133*, 647–658.

Received: March 2, 2016
Revised: May 7, 2016
Published online: June 21, 2016

